Published in final edited form as:
Nano Lett. 2010 December 8; 10(12): 5098–5102. doi:10.1021/nl1035447.

Plastic deformation drives wrinkling, saddling and wedging of annular bilayer nanostructures

Jeong-Hyun Cho[*], **Dibakar Datta**[**], **Si-Young Park**[*], **Prof. Vivek B. Shenoy**[**], and **Prof. David H. Gracias**[*,#]

Vivek B. Shenoy: vivek_shenoy@brown.edu; David H. Gracias: dgracias@jhu.edu

[*] Department of Chemical and Biomolecular Engineering, Johns Hopkins University, Baltimore, MD 21218, USA

[**] School of Engineering, Brown University, Providence 02912, USA

[#] Department of Chemistry, Johns Hopkins University, Baltimore, MD 21218, USA

Abstract

We describe the spontaneous wrinkling, saddling, and wedging of metallic, annular bilayer nanostructures driven by grain coalescence in one of the layers. Experiments revealed these different outcomes based on the dimensions of the annuli and we find that the essential features are captured using finite element simulations of the plastic deformation in the metal bilayers. Our results show that the dimensions and nanomechanics associated with the plastic deformation of planar nanostructures can be important in forming complex three dimensional nanostructures.

Keywords

self assembly; self folding; nanomechanics; lithography; buckling

Nature is replete with structures such as leaves, flowers, insect wings, animal horns, skin, and sea shells that display complex curvatures.[1] Hence, an understanding of processes that drive spontaneous curving of planar structures into unique three dimensional geometries is important in rationalizing and mimicking naturally occurring assembly processes. A number of recent research studies have focused on understanding mechanisms that enable the spontaneous transformation of two dimensional structures into curved three dimensional structures.[2–17] These studies have often involved the utilization of materials with non-uniform composition or thin-film based mis-matched bilayers. For example, Klein et al, have studied the thermal shrinkage of non-uniform thin gel sheets composed of n-isopropylacrylamide (NIPA) gels and observed numerous spontaneously formed wavy structures. [2] Mahedevan and Rica have shown that stresses induced by thermal or desiccating effects of stiff materials on soft supports result in folds that are reminiscent of those observed on leaves.[3] Bowden et al, have observed the spontaneous formation of wavy micro patterns when metals were evaporated onto polydimethylsiloxane.[4]

On the micro and nanoscale, spontaneous curving is also important for the synthesis of three dimensional structures that cannot be readily fabricated by conventional planar lithographic processes. Self-assembly methods can be used in combination with precise and well developed 2D lithographic processes such as photo, e-beam, and nanoimprint lithography to generate simultaneously curved and patterned micro and nanostructures. There have been

Correspondence and requests for materials should be addressed to D.H.G. (dgracias@jhu.edu).

two predominant strategies that have been shown to generate the high stresses required to curve structures with nanoscale radii. These include the stress generated by grain coalescence[8–10] and heteroepitaxy.[14–17] These methods have been utilized to generate a range of structures (e.g. cylinders) typically with intuitive outcomes such as uni-directional curvature. In order to generate more complex, non-intuitive assemblies, such as that observed in nature, we focus on an investigation of the mechanics of self-assembly based on plastic deformation associated with grain coalescence within annular bilayers.

Here, we systematically investigated self-assembly outcomes from a single geometry (annular shaped bilayers), and identical composition [nickel (Ni)/tin (Sn)], while varying only the lateral and vertical dimensions. Grain coalescence was induced in the tin layer and the stress associated with this plastic deformation drove spontaneous assembly of complex 3D structures with both uni and bi-directional curvature. The formation of these nanoscale structures was experimentally demonstrated as well as modeled using finite element methods. Here, the same initial planar annular shape but with different dimensions resulted in the formation of dramatically different and complex 3D structures on assembly. The 3D structures were wrinkled, saddled, or wedged shaped. One assembly outcome that we find particularly interesting is the saddling-type transformation reminiscent of a bifurcation or symmetry breaking transformation. This transformation results in spontaneous assembly of a structure with bidirectional curvature. The design of structures that display nanomechanical bifurcations remains challenging. Additionally, our assemblies resemble buckling transformations that are widely thought to be associated with mechanism of rapid closing of naturally occurring macroscale mechanical structures such as the Venus Fly Trap.[18–20]

Figure 1 illustrates our concept of patterning an annular bilayer and driving assembly based on grain coalescence. Ni and Sn layers are deposited and patterned into annular shapes on a (silicon) Si substrate (Figure 1a, b). The Sn film deposits with a grainy morphology due to the intermediate wetting tendency of Sn on Ni.[8–10] During etching of the underlying Si substrate with a plasma etcher, the annular bilayer is simultaneously released from the Si substrate and also heated due to the exothermic chemical reactions associated with etching. This heat induces grain coalescence in Sn as a consequence of which a stress is generated within the Sn film.[9–10] This stress associated with plastic deformation generates a large differential stress in the Ni/Sn bilayer driving spontaneous assembly (Figure 1c, d) with nanoscale curvature. Once, formed the structures remain frozen in their self-assembled or deformed state.

Annular patterns with different dimensions were defined in a 100 nm thick electron-beam (e-beam) resist. Briefly, polymethylmethacraylate (PMMA, MW 950K A2), was spun on an n-type <100> bare silicon (Si) wafer, and the wafer was baked at 185 °C for 3 minutes. An e-beam controlled by a RAITH system (Quantum v 4.0) was used to pattern the resist with annular patterns with varying widths (w) and diameters. The smallest width and inner diameter of the annuli were 25 nm and 200 nm, and the largest width and inner diameter were 800 nm and 4000 nm, respectively. After e-beam patterning, the resist was developed using an MIBK developer (MIBK:IPA = 1:3) for 35 seconds. Then, a 0.2 nm chromium (Cr) adhesion layer and the respective thickness (5, 10, and 20 nm) of Ni were deposited using a thermal evaporator. On the top of the sample, the required thickness of Sn (2.5, 5, 10, and 20 nm) was thermally evaporated. After evaporation, the e-beam resist was dissolved in acetone for about 30 minutes to achieve lift-off metallization. E-beam patterned samples were loaded in a planar plasma etcher (Technics PEII-A) at a base pressure of 0.15 Torr. Carbon tetrafluoride (CF_4) and oxygen (O_2) were flowed into the etcher with flow rates of 12 and 3.6 sccm respectively for 3 minutes after which 25W RF power was applied for 4 minutes. Self-assembly occurred during etching of the underlying Si substrate within the plasma

etcher; we made sure that the structures were etched long enough so as to completely release the structure from the underlying substrate.

The deformation of the annular bilayer structures was modelled using the finite element method (FEM), with a shell element made up of two layers (Sn on top of Ni) of materials. To model the stresses induced by coalescence we assumed an equi-biaxial strain in the Sn layer. This is a reasonable assumption since the in-plane dimension of the film-substrate system is much larger than its total thickness.

The equi-biaxial stress in Sn can be computed using the relation[21],

$$\sigma_m = \varepsilon_m M_f \quad (1)$$

Here ε_m is the mismatched strain between the film and the substrate and M_f is the biaxial modulus of the film material given by

$$M_f = E_f/(1-\nu_f), \quad (2)$$

The values of the Young's modulus (E_f) and Poisson's ratio (ν_f) used for Ni and Sn were 200 GPa, 50 GPa and 0.31, 0.36 respectively and the mismatch strain was 0.07. With this mismatch strain, we obtained an equi-biaxial stress σ_m =5.5 GPa. This stress is very high and consistent with plastic deformation. We treated the plastic deformation of the metals using a power Law type strain hardening relation given by

$$\sigma = \sigma_y + K\varepsilon_p^n \quad (3)$$

where K = 2 GPa (strength index), n = 0.3 (strain hardening index) assumed to be same for both Ni and Sn, σ_y is the yield stress (0.010 GPa for Sn and 0.025 GPa for Ni.[22]), ε_p is the plastic strain and σ is the stress.

In FEM simulations, we first carried out a linear buckling analysis to obtain the buckling modes. These modes were then applied as an initial perturbation to the annulus and the FEM simulations were used to carry out the post buckling non-linear analysis to determine the final deformed shapes. All simulations were carried out in a finite deformation setting; i.e., the effect of geometric changes on the force balance and the rigid body rotations were explicitly taken into account.

Figure 2 shows SEM images of the annular patterns after two-dimensional (2D) patterning (Figure 2a) and the same patterns after plasma etching (Figure 2b, with zoomed images in Figure 2c–e). The associated FEM results are shown in Figure 2f–h. All 2D patterns had the same diameter (d_M) of 3 microns and were composed of a bilayer with a thickness of 5 nm for both Ni and Sn. The only variable was the width (w) of the annulus which was varied between 600 nm to 75 nm (Figure 2a). After self-assembly, three distinct nanostructures were observed (Figure 2b); (i) wrinkled nanostructures (w = 600 nm, Figure 2c, f) which were structures with wrinkled side walls. It should be noted that in all cases, only the outer edge of the annulus was wrinkled while the inner one was uniformly curved, (ii) saddle-shaped nanostructures (w = 300 nm, Figure 2d, g), which were annuli where circular symmetry was broken and a consequence of a bifurcation with bi-directional curvature, and (iii) wedged annuli (w = 150 and 75 nm, Figure 2e, h) where the side wall of the annulus was sloped with a spherical shape. In all wedged nanostructures the slope was negative towards the center of the annulus. It should be noted that our results were highly

reproducible as was verified on multiple samples both on the same wafer and in multiple runs.

We can rationalize the general trends from the bifurcation analysis of circular discs which is discussed in reference [21]. Here for small radii, the disc deforms into a shape whose two principal curvatures are equal i.e. into a section of a spherical surface as shown in Figure 2e and h. However, above a certain size (or bifurcation point in mathematical terms) it becomes energetically favorable to form a shape that is predominantly curved in one direction, or one that resembles a cylinder. The saddle-shaped structures (Figure 2d, g) are formed during this transition. The bifurcation is indeed what we find in our simulations. For small widths, the wedge shape seen in Figure. 2e–h is the section of spherical surface with equal curvatures in the two directions. With increasing widths, the annuli tend to curve into cylinders with the radii of the cylinders decreasing with increasing widths. Saddle-shaped structures (Figure 2d, g) are formed in between. When the radii of the cylinders becomes comparable to the mean diameter of the annulus, wrinkled structures such as ones seen in Figure 2c and f are obtained.

As this cylinder radius becomes small, polygonal wrinkled shapes such as the ones shown in Figure 3 are seen. In this case, each section of the annulus is trying to fold into a cylinder, but given its circular shape, this can only be accomplished by formation of the polygonal shapes where each segment assumes an approximately cylindrical shape. The number of edges (N_e) of this polygon formation depends on width and diameter. Experimental results of the annuli (d_M = 2 μm and w = 400 nm) show that N_e = 7~8 (Figure 3a) with a corresponding modeling result N_e = 7 (Figure 3c). Our simulation also shows good agreement with the annuli which have a 4 μm diameter (d_I) with varying widths (w) from 800 to 100 nm (Figure 3d, e). Figure 3e shows models of the annuli shown in Figure 3d. It turns out that the number of edges decreases when width decreases (Figure 3d, e). We also observed that only outer edge wrinkles but the inner edge is uniform as it is energetically favorable shape (Figure 3g, h)

We noticed that the bifurcation and the formation of saddle shaped structures also depends in a significant way on the thickness of the metals (Figure 4a–f) as well as the diameter of the annulus (Figure 4g–l). Annular patterns curved more when the thickness of the Ni film was decreased and when their overall diameter was reduced. The radii of curvature variations are in agreement with previous experimental results on cantilever shaped structures.[9]

In conclusion, this study shows how plastic deformation can be utilized to drive assembly of complex 3D nanostructures. Using both experiments and simulations we highlight a large number of assembly outcomes based on the same initial annular shape but with variable dimensions. As compared to elastic forces, the strain associated with plastic deformation can be large and drive irreversible assembly with extremely small nanoscale radii of curvature. These radii are challenging to achieve using intrinsic stresses, whose magnitude tends to be on the order of 1GPa, even in highly stressed metals such as chromium.[23] Another significant result is the creation of saddled-shaped nanostructures that are reminiscent of “potato-chip” like structures with a spontaneous bifurcation and two bi-directional radii of curvature.[2] Moreover, elucidating pathways of plastic deformation of nanostructures is important in understanding structural and failure properties of nanostructured materials and devices. Apart from the intellectual importance of this study, we also believe that these nanostructures, when composed of dielectrics such as alumina and patterned with metals, silver or gold, could display novel electromagnetic and structural properties. Here, it is noteworthy that patterning can be done with high precision in 2D, while enabling the formation of 3D nanostructures.

Acknowledgments

This research was supported by the NIH Director's New Innovator Award Program, part of the NIH Roadmap for Medical Research, Grant No. 1-DP2-OD004346-01 and by the National Science Foundation (NSF) Grant No. 0854881. V.B.S. gratefully acknowledges support from the NSF through Grants CMMI-0855853, DMS-0914648, and DMS 0854919.

References

1. D'Arcy, WT. On Growth and Form: The Complete Revised Edition. Dover Publications; New York: 1992.
2. Klein Y, Efrati E, Sharon E. Science. 2007; 315:1116–1120. [PubMed: 17322058]
3. Mahadevan L, Rica S. Science. 2005; 307:1740. [PubMed: 15774751]
4. Bowden N, Brittain S, Evans AG, Hutchinson JW, Whitesides GM. Nature. 1998; 393:146–149.
5. Syms RRA, Yeatman EM. Electron Lett. 1993; 29:662–664.
6. Gracias DH, Kavthekar V, Love JC, Paul KE, Whitesides GM. Adv Mater. 2002; 14:235–238.
7. Gimi B, Leong T, Gu Z, Yang M, Artemov D, Bhujwalla ZM, Gracias DH. Biomed Microdevices. 2005; 7:341–345. [PubMed: 16404512]
8. Cho JH, Gracias DH. Nanolett. 2009; 9:4049–4052.
9. Cho JH, James T, Gracias DH. Adv Mater. 2010; 22:2320–2324. [PubMed: 20376856]
10. Cho JH, Azam A, Gracias DH. Langmuir. 2010; 26:16534–16539. [PubMed: 20507147]
11. Leong TG, Zarafshar AM, Gracias DH. Small. 2010; 6:792–806. [PubMed: 20349446]
12. Py C, Reverdy P, Doppler L, Bico J, Roman B, Baroud CN. Phys Rev Lett. 2007; 98:156103. [PubMed: 17501365]
13. Patra N, Wang B, Kral P. Nano Lett. 2009; 9:3766–3771. [PubMed: 19852466]
14. Prinz VY, Seleznev VA, Gutakovsky AK, Chehovskiy AV, Preobrazhenskii VV, Putyato MA, Gavrilova TA. Physica E. 2000; 6:828–831.
15. Schmidt OG, Eberl K. Nature. 2001; 410:168. [PubMed: 11242068]
16. Mei Y, Thurmer DJ, Deneke C, Kiravittaya S, Chen YF, Dadgar A, Bertram F, Bastek B, Krost A, Christen J, Reindl T, Stoffel M, Coric E, Schmidt OG. ACS Nano. 2009; 3:1663–1668. [PubMed: 19552386]
17. Schmidt OG, Schmarje N, Deneke C, Muller C, Jin-Phillipp NY. Adv Mater. 2001; 13:756–759.
18. Forterre Y, Skotheim JM, Dumais J, Mahadevan L. Nature. 2005; 433:421–425. [PubMed: 15674293]
19. Volkov AG, Adesina T, Markin VS, Jovanov E. Plant Physiol. 2008; 146:694–702. [PubMed: 18065564]
20. Holmes DP, Crosby AJ. Advanced Materials. 2007; 19:3589–3593.
21. Freund, LB.; Suresh, S. Thin Film Materials: Stress, Defect Formation and Surface Evolution. Cambridge University Press; Cambridge: 2004. p. 87-91.p. 132-142.
22. Howatson, AM.; Lund, PG.; Todd, JD. Engineering Tables and Data. 2. Kluwer Academic Publishers; Dordecht: 1991. p. 41
23. Tyagi P, Bassik N, Leong TG, Cho JH, Benson BR, Gracias DH. J Microelectromech Sys. 2009; 18:784–791.

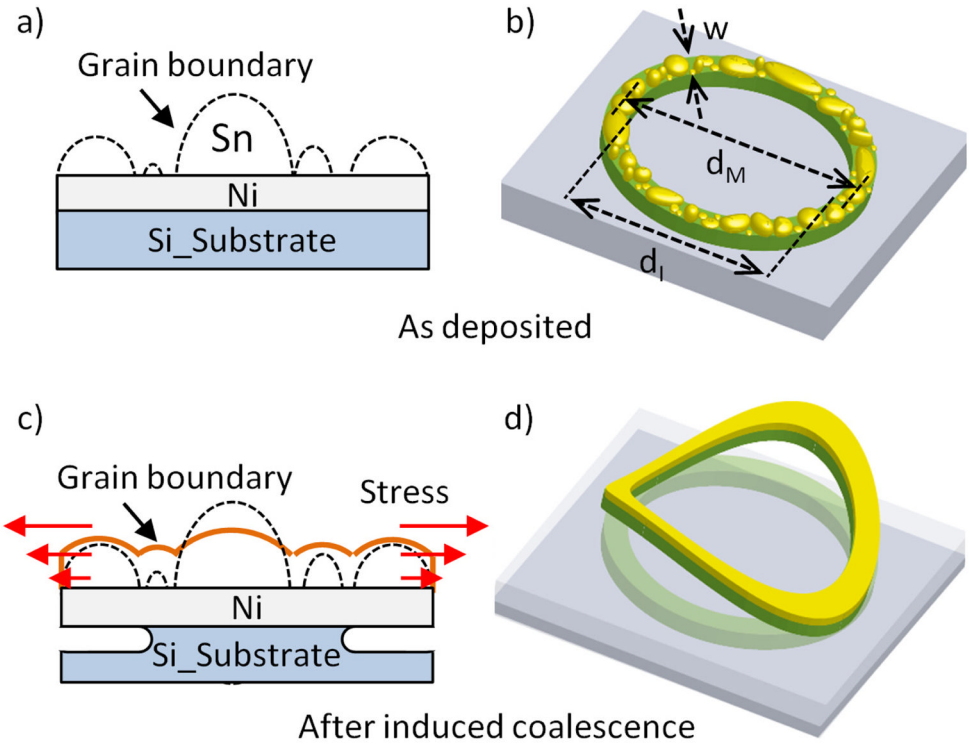

Figure 1.
Schematic diagram showing the concept of the spontaneous formation of complex 3D nanostructures driven by plastic deformation of annular bilayers. (a) Side and (b) angled view of an annulus as fabricated on a silicon substrate with Sn deposited atop of Ni. (c) Side and (d) angled view of a saddle-shaped nanostructure that forms spontaneously after assembly and is driven by Sn grain coalescence.

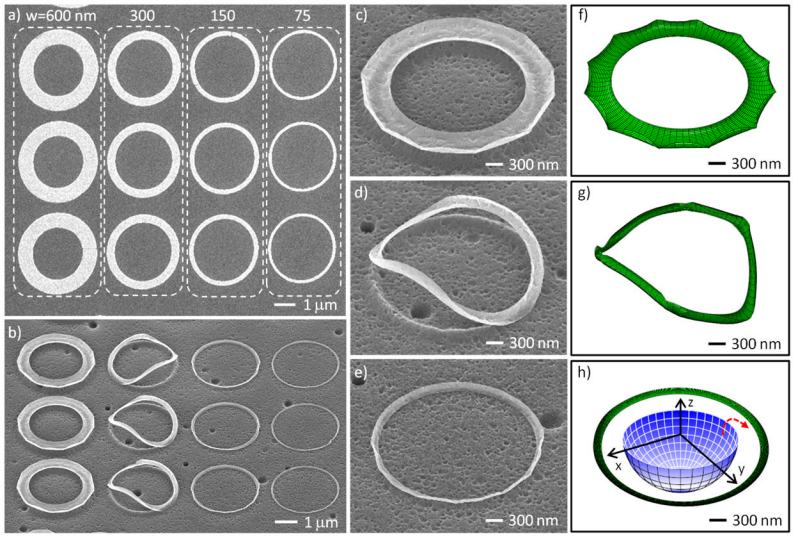

Figure 2.

Self-assembly of wrinkled, saddled, and wedged shaped nanostructures. All structures have the same diameter (d_M) of 3 microns and were composed of a bilayer with a thickness of 5 nm for both Ni and Sn. (a, b) SEM images of annular annuli with widths of 600, 300, 150, and 75 nm; (a) as patterned top view, and (b) after self-assembly with a 50 degrees tilted view. (c–e) Zoomed-in SEM images of a single (c) wrinkled with w = 600 nm, (d) saddled with w = 300 nm, and (e) wedged nanostructure with w = 150 nm. (f–h) FEM images of the corresponding (f) wrinkled, (g) saddled, and (h) wedged annular nanostructures. The inset in panel (h) is a schematic of a section of a spherical surface with equal curvatures in both directions.

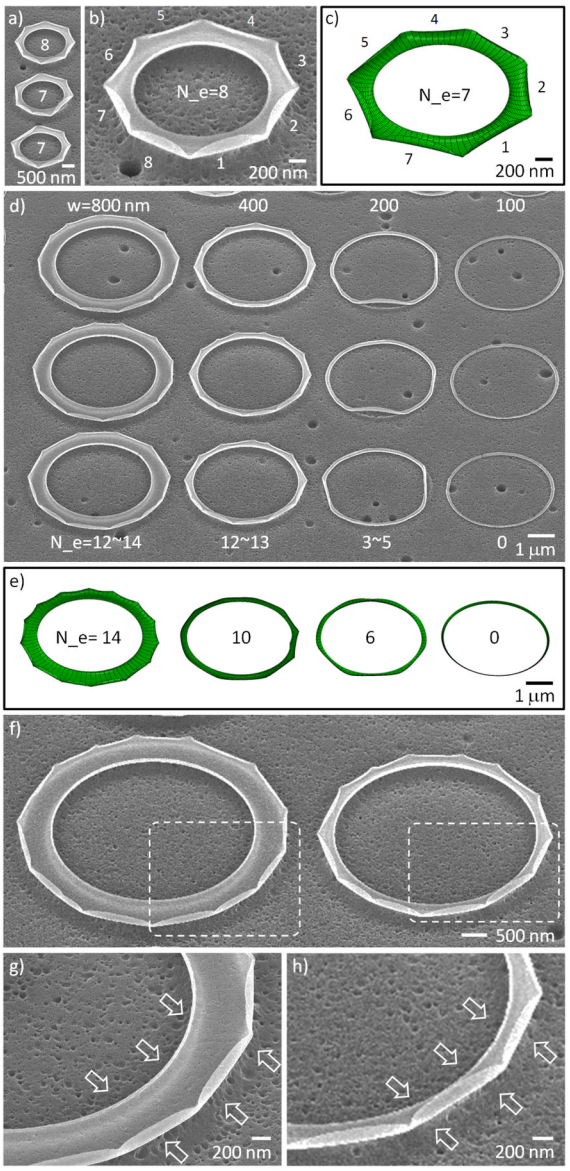

Figure 3.

Variation in the number of edges formed during assembly of wrinkled nanostructures. SEM images of nanostructures with (Ni 5/Sn 2.5 nm) with varying diameter and widths. (a–c) SEM and FEM results of annular structures with the same diameter (d_M) of 2 μm and width (w) of 400 nm. (a) SEM images show that the structures assemble with the number of edges of polygon formation N_e = 7~8. (b) Zoomed-in image of one of wrinkled nanostructure shown in (a) with N_e = 8. (c) FEM result showing corresponding wrinkling with N_e = 7 and in good agreement with experiments. (d, e) Variation of number of wrinkles with the same inner diameters (d_I) of 4 μm and varying width (w) of 800, 400, 200, and 100 nm. (d) SEM images show that the assembly in an array with N_e decreasing with decreasing width so that N_e = 12~14 for a width of 800 nm and N_e = 0 for a width of 100 nm. (e) FEM results are in reasonable agreement with the experiments based on the N_e predicted for different geometeries. (f) SEM images of two annuli (w = 800 and 400 nm) showing that wrinkling occurs only on the outer edge of the annulus, while the inner edge is uniformly curved. (g, h) Zoomed-in images of the wrinkled nanostructures shown in (f)

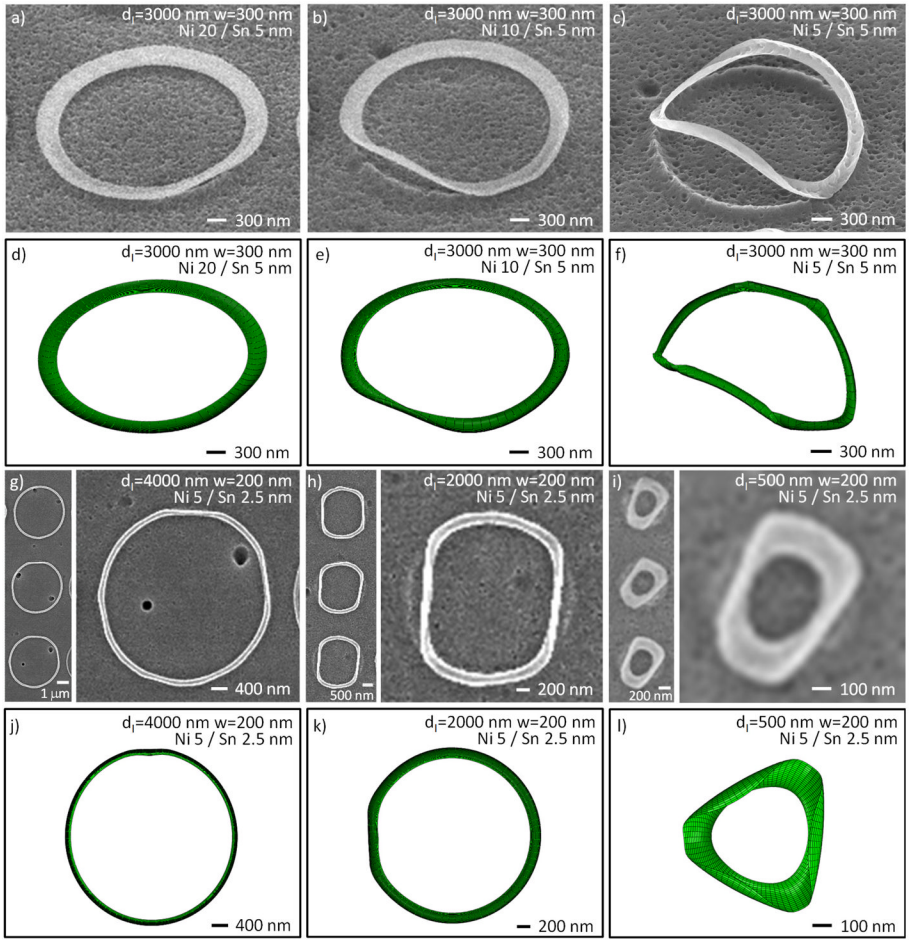

Figure 4.

Variation of the onset of saddling in nanostructures with different thickness and diameter. In addition to the width of the annulus, the saddling of the nanostructures is also affected by (a–f) the thickness of the bilayer annular films as well as (g–l) their diameter. (a–f) SEM and FEM images of annuli with the same diameter (d_I) = 3000 nm, width (w) = 300 nm, and variable thickness of (a, d) Ni 20 nm/Sn 5 nm, (b, e) Ni 10 nm/Sn 5 nm, and (c, f) Ni 5 nm/Sn 5nm. The sequence of images shows that the onset of saddling depends on the thickness of the films. (g–l) SEM and FEM images of annuli with the same film thickness of Ni 5 nm/Sn 2.5 nm, width (w) = 200 nm, and variable diameters (d_I). (g, j) d_I = 4000 nm. (h, k) d_I = 2000 nm. (i, l) d_I = 500 nm. The sequence of images shows that the onset of saddling depends on the diameter of the annulus.